

A Comparison of Mid-Level Frontogenesis to Radar-Indicated Heavy Snowbands

CHRISTOPHER D. KARSTENS

Iowa State University, Ames, Iowa

Mentor: Dr. William A. Gallus Jr.

Iowa State University, Ames, Iowa

ABSTRACT

Frontogenesis and conditional symmetric instability have been researched extensively, becoming widely used as a means of predicting small scale heavy snow events. The secondary ageostrophic circulation induced by frontogenesis has been shown to produce narrow bands of precipitation, sustained for periods of time by the continual release of moist symmetric instability. This study analyzes six levels of frontogenesis to determine if a specific level is consistently in close proximity to the radar-indicated snowband detected at the same time. The closest level for three cases was examined in greater detail to emphasize a relationship between frontogenesis and moist symmetric instability. Results show frontogenesis in the 700mb to 750mb layer was close to the snowband location within reasonable accuracy, but is shown to vary. In addition, two conceptual models of frontogenesis in relation to saturated equivalent potential vorticity are verified.

1. Introduction

Several dynamical forcing mechanisms have been identified and researched to explain the occurrence of mesoscale precipitation bands in winter cyclonic storms (Shields et al. 1991). These include conditional symmetric instability (CSI) (Bennetts and Hoskins 1979; Emanuel 1983a,b; Schultz and Schumacher, 1999), frontal circulations (Browning and Harrold 1970), isentropic lift (Moore 2006), troughs associated with occluded cyclones (Martin 1999), gravity wave propagation within atmospheric ducts (Lindzen and Tung 1976), geostrophic deformation and the accompanying transverse ageostrophic circulation (Eliassen 1962), boundary layer convergence (Hobbs et al. 1980), vertical shear instability in the middle troposphere above cold frontal zones (Wang et al. 1983), melting induced circulations (Szeto et al. 1988), and stationary gravity waves near frontal boundaries (Gall et al. 1988). Among these, frontal circulations have been shown to

produce and sustain narrow bands of precipitation in regions of frontogenetic forcing (Banacos 2003).

Frontogenesis is defined as the initial formation of a front or frontal zone, caused by an increase in the horizontal gradient of an air mass property, principally density, and the development of the accompanying features of the wind field that typify a front (American Meteorological Society 2006). Deformation, the process by which an air stream stretches or alters the distribution of elements embedded in the flow, can lead to the formation of frontogenesis and the focusing of precipitation into narrow bands (Moore 2006). The frontogenesis parameter is a function of how perpendicular contrasting air masses are to the wind flow and varies spatially with time.

Frontogenesis and CSI have been researched extensively and have become widely used as a means of predicting small scale heavy snow events. Sanders and Bosart (1985), Sanders (1986), and Wolfsberg et al. (1986) all showed

that frontogenesis and CSI (and/or low moist symmetric stability) were present during major northeastern United States snowstorms that possessed mesoscale snowbands. Furthermore, Emanuel (1985) considered a coupled dynamical relationship for producing mesoscale precipitation bands between frontogenesis and moist symmetric instability (MSI). Emanuel showed that on the warm side of a developing frontal zone when symmetric stability was low, ascent associated with frontogenesis was enhanced and constricted to a smaller scale. In addition, Xu (1989) showed that long-lived mesoscale precipitation bands are theoretically the result of frontogenesis in the presence of CSI (Nicosia and Grumm 1999). An outbreak of research on CSI came in the 1990s in which several papers misuse CSI. Schultz and Schumacher (1999) address this issue by stating saturated theta-e should be used in assessing regions of CSI rather than theta-e. To diagnose regions of CSI, saturated equivalent potential vorticity (EPV*) can be used in a baroclinic atmosphere. Schumacher (2003) showed EPV* values less than 0.25 PVU to be associated with banded precipitation through operational research.

The location of the snowband in relation to frontogenesis has been shown to vary. Banacos (2003) suggests the identification of a col point, either in profiler data or model forecasts, can be used as a signal to the occurrence of banding precipitation. This should be further evaluated by explicit examination of the frontogenesis/deformation field. The level at which the col point is located determines which level of frontogenesis that should be used to forecast banded precipitation.

In addition, Nicosia and Grumm (1999) takes the research of Sanders, Bosart, Wolfberg, Emanuel, and Xu, among others, into account in assessing three major winter storms producing heavy snowbands in the northeast United States. Cross-sectional analyses (oriented perpendicular to the isotherms) were used to indicate that mesoscale snowbands formed in a *deep layer of negative EPV directly above strong mid-level frontogenesis* (Fig. 1(a)). Banacos 2002 has a slightly different view, stating that instability is likely released as rapidly as it is created, due to the lift associated with frontogenesis occurring to produce the instability. Therefore, regions of CSI are *unlikely* to appear above frontogenesis (Fig. 2(b)). Both of these ideas

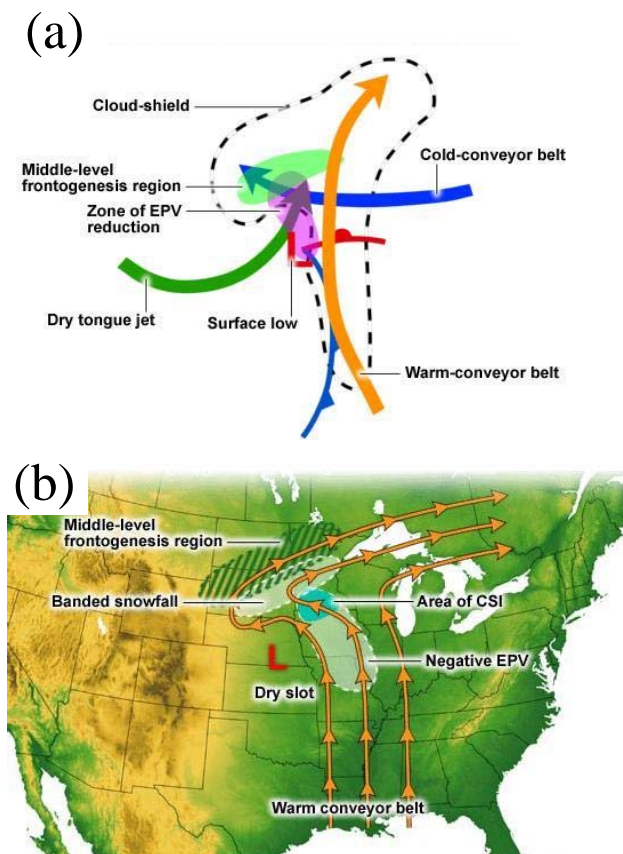


Fig 1. Conceptual model of frontogenesis and CSI from (a) Nicosia and Grumm (1999) and (b) The Comet Program.

include the presence of mid-level frontogenesis to realize the instability.

However, an inconsistency among much research involving frontogenesis is the level or layer used in verifying and predicting heavy snow events. Experts have used levels ranging from the surface to 500mb, and various layer averaging of frontogenesis. Banacos (2003) states that frontogenesis at 700mb is perhaps most often aligned with banded precipitation, but was shown to vary within the 500mb to 850mb range. *My hypothesis is the 600mb to 850mb range will consistently indicate a correlation between frontogenesis and reduced EPV* when mesoscale snowbands are detected on Doppler radar.* My study will examine the frontogenesis parameter at 50mb increments from 850mb to 600mb. Saturated EPV* will be examined in the 100mb to 150mb layer directly above the frontogenesis level closely correlated with the snowband to determine whether CSI exists in this region. To do this, GEMPAK will be used to analyze the 80-km Eta/Nam Model, and diagnose frontogenesis and CSI/EPV* in proximity to the mesoscale snowbands detected

by WSR-88D data and verified by local observations. Ten cases confined to the upper Midwest are examined, and three representative cases are analyzed in further detail. In each case, the cause for the enhanced snowband is investigated.

2. Data and Methodology

Frontogenesis was examined using the Eta/Nam model, and was compared to WSR-88D radar data valid at the same time. Data was collected for ten snowstorms occurring across the upper-midwest. The snowstorms occurred on the following dates and locations: January 26, 1996 in Iowa and Wisconsin, January 29-30, 2001 in South Dakota and Minnesota, November 26-27, 2001 in South Dakota and Minnesota, January 29-30, 2001 in South Dakota, December 23-24, 2002 in Missouri, February 23-24, 2003 in Kansas and Missouri, March 15-16, 2004 in Iowa, March 18-19, 2005 in South Dakota and Minnesota, November 28-29, 2005 in Nebraska and South Dakota, and March 16, 2006 in South Dakota and Minnesota. Cases were selected on the criteria of data availability and precipitation focused into concentrated snowbands.

WSR-88D radar data were analyzed using base reflectivity data from the 0.5° elevation, obtained from the Iowa Environmental Mesonet (IEM), the University Corporation for Atmospheric Research (UCAR), and the National Climatic Data Center (NCDC). Composite radar imagery was available for seven of the ten cases to provide a larger perspective of the snowstorm for improved model comparison. Surface observations, cooperative snow observations, and official National Weather Service (NWS) observations were used to verify radar reflectivity. Data were obtained from the IEM and The Pennsylvania State University meteorological system.

The Eta/Nam model was examined using GEMPAK. The model forecasts were available every 12 hours for all ten cases. Thus, initializations were used and 6-hour forecasts were needed for analysis of the 06Z and 18Z time periods. Forecast errors should be relatively small at six hours. Six levels of frontogenesis were analyzed, including 600mb, 650mb, 700mb, 750mb, 800mb, and 850mb (Nicosia and Grumm 1999). Frontogenesis was calculated from GEMPAK using potential

temperature and the total wind (geostrophic plus ageostrophic). Potential temperature was used instead of temperature to more accurately describe frontogenesis in areas where terrain could have an influence. In addition, it has been shown that in strong frontal zones, the ageostrophic component of the wind is important. Thus, the total wind was used rather than geostrophic winds alone.

Radar data showing banded areas of reflectivity, valid at the same time, were collected to investigate which level of frontogenesis aligned closest to the radar-indicated snowband. This was accomplished by transcribing the snowband on the six concurrent levels of frontogenesis. The distance was determined by measuring from the snowband perpendicularly in the direction of the frontogenesis maximum for each level. When the snowband occurred on the warm side of the frontogenesis maximum, the distance was positive. Negative distances were assigned when the snowband was on the cold side of the frontogenesis maximum. The snowband, therefore, was positioned at 0km. This was conducted for each case when a snowband was detected by radar at the model initialization and six hour forecast time periods, yielding 38 total time periods for analysis.

EPV* was also calculated using saturated theta-e and the full wind over a layer average in GEMPAK. Values of $2.5E-07 \text{ sec}^{-1}$ (0.25 PVU) and less, at $0.5E-06 \text{ sec}^{-1}$ (0.5 PVU) intervals, were overlaid onto composite radar imagery and frontogenesis valid at the same time. The 100mb to 150mb layer directly above the level of frontogenesis closely correlated to the snowband was used to verify the validity of the conceptual models presented in Fig. 1.

3. Case Overview and Analysis

Three representative cases from the cumulative data set were chosen for detailed analysis. These include November 26-27, 2001, March 15-16, 2004, and March 17-18, 2005. Collectively these cases illustrate a number of common synoptic elements typically associated with winter storms in the upper Midwest. The evolving impacts of these features are analyzed.

a. November 26-27, 2001

A narrow band of twelve to eighteen inches of snow stretched across southern South Dakota, central Minnesota, and northern Wisconsin. The storm came into fruition in central Minnesota where amounts exceeded two feet in several locations (Fig. 2(a)). Four time periods, from 06Z on the 26th to 00Z on the 27th, were available and used for this case.

At 06Z on the 26th, a surface low was located in southwestern Kansas, with strong warm air advection occurring ahead of it. At 500mb the low was cutoff, imbedded within a negatively tilted trough. These features were associated with the left exit region of an upper-level trough. Radar indicated a narrow band of snow from north-central Nebraska northeastward into southeast South Dakota. The 700mb frontogenesis closely resembled the snowband, as it was positioned directly on top of the snowband. The 750mb maximum was positioned close as well, 28km south of the snowband (Fig 2(b)).

The snowband shifted slightly to the north into southern South Dakota by 12Z. Frontogenesis at this time shifted a bit further to the north as well. The surface low moved into north central Kansas at this time. The 750mb and 800mb frontogenesis maxima were closest

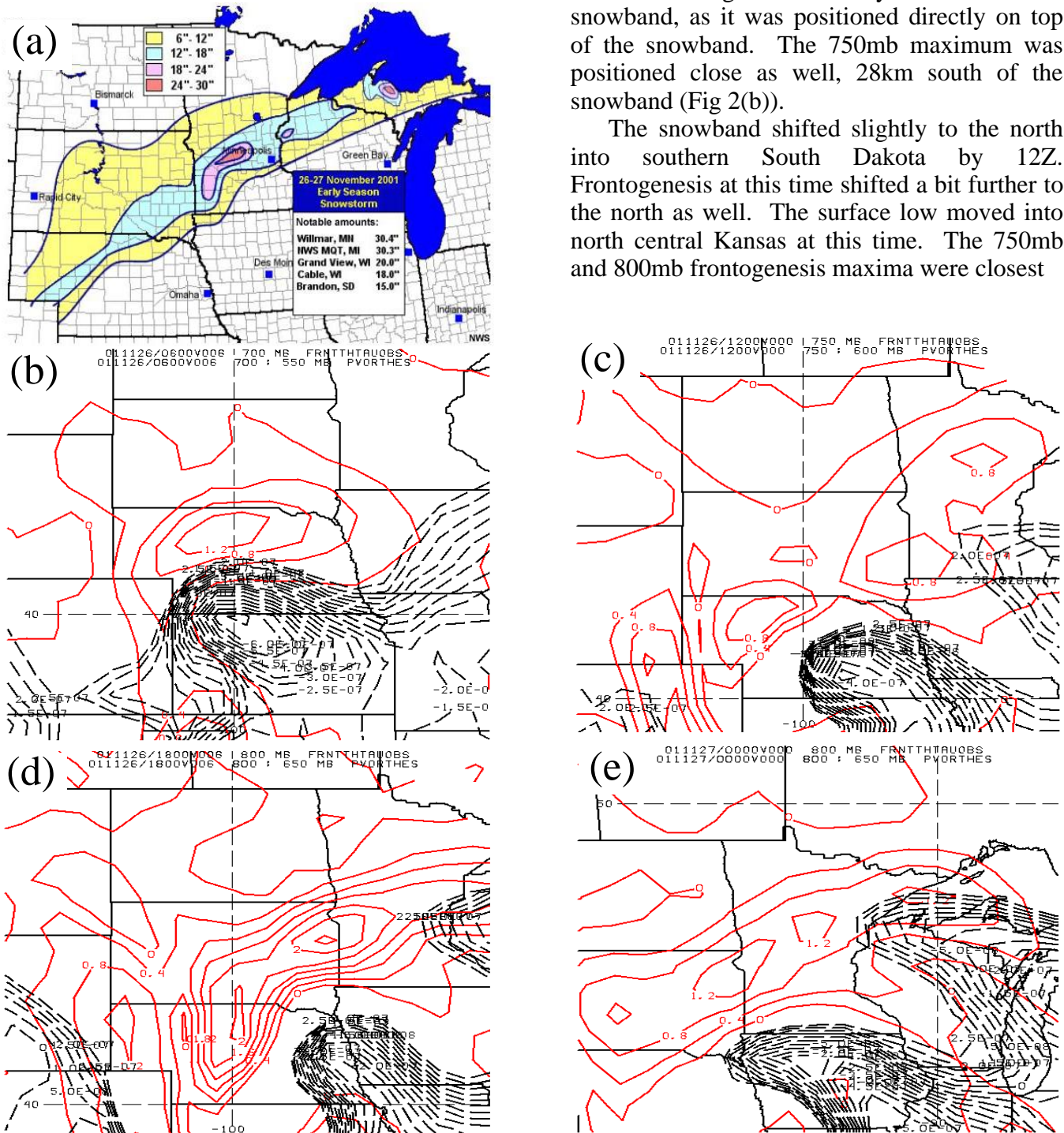


Fig. 2. (a) Total snowfall (in) for 26 and 27 Nov 2001 across the upper midwest. Contour interval every 6in. (Moore 2006), (b) frontogenesis (line contours, K/100km/3hr) and EPV* (sec⁻¹) less than 0.25 PVU valid 26 Nov 2001 at 06Z, (c) 12Z, (d) 18Z, and (e) 27 Nov 2001 at 00Z.

to the snowband, slightly lower in the atmosphere than seen at 06Z. Distances were 28km to the north and south respectively (Fig. 2(c)).

At 18Z, the frontogenesis in the upper four layers was displaced well away from the snowband into northern Minnesota. Radar indicated a snowband persisting in southern South Dakota and intensifying in central Minnesota. The surface low continued its northeasterly track, positioned in northeastern Kansas and southeastern Nebraska. The 800mb and 850mb frontogenesis was rather intense and well correlated with the snowband. Once again, lower levels were in better agreement with the snowband location than previously indicated (Fig. 2(d)).

The snowband bisected central Minnesota at 00Z on the 27th. Surface low pressure was centered along the Nebraska-Iowa boarder. Though still rather disorganized, the frontogenesis in the upper layers showed better alignment with the snowband location than

before. 700mb frontogenesis was nearly on top of the snowband once again. Strong frontogenesis was also still present at 800mb and 850mb. This case showed that frontogenetic forcing from 700mb to 850mb at different time periods may have assisted in sustaining the mesoscale snowbands (Fig. 2(e)).

This case showed how the distance from the snowband to the closest frontogenesis maximum can vary greatly in successive time periods. In addition, EPV* in the 150mb layer above the closest frontogenesis is consistently located to the southeast of the frontogenesis and snowband, validating the conceptual model presented in Fig. 1(b).

b. March 15-16, 2004

This snow event occurred across central sections of Iowa, where a constricted band of ten to sixteen inches of snow accumulated (Fig. 4). Four time periods, from 12Z on the 15th through 06Z on the 16th, were used for analysis.

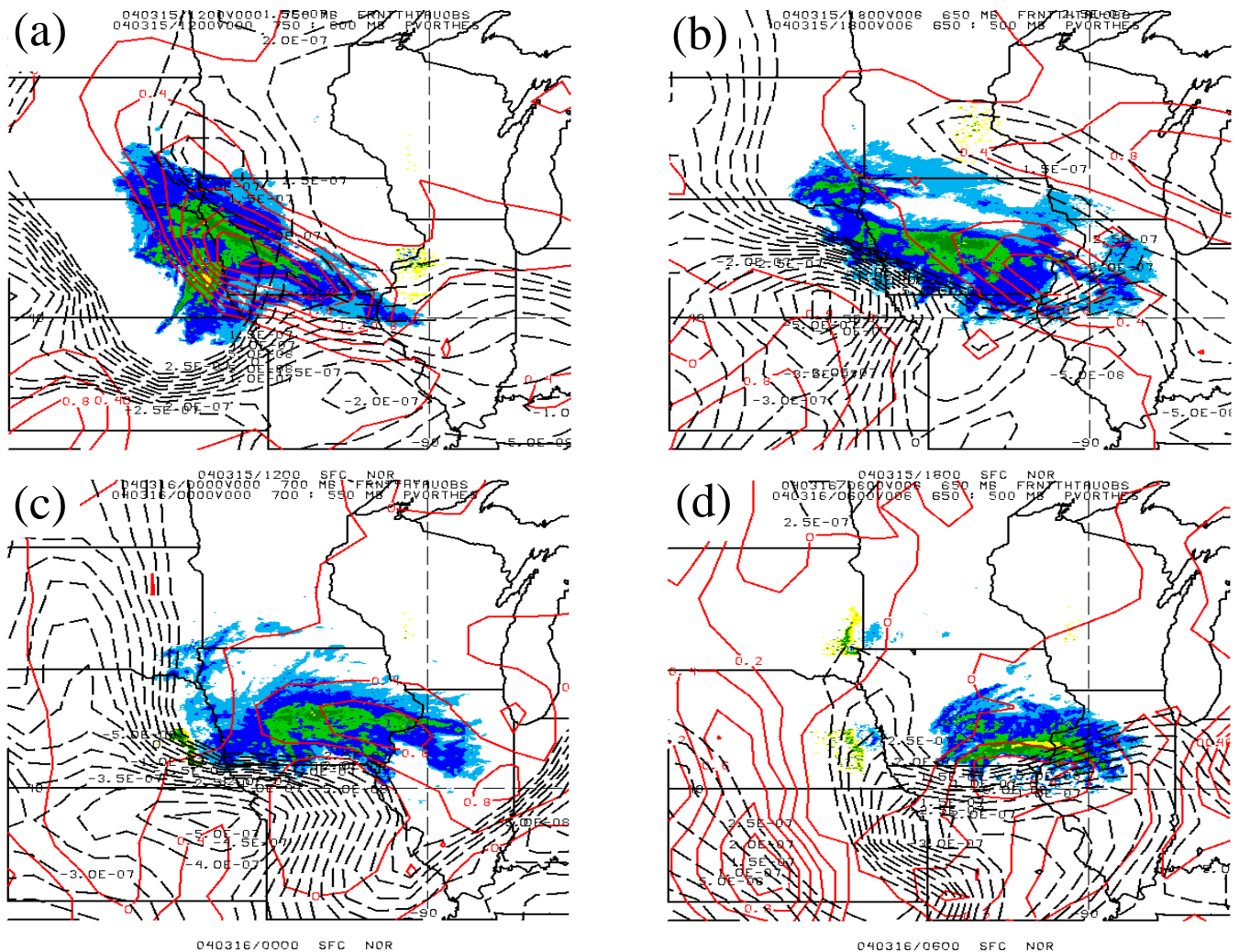


Fig. 3. Composite Radar Imagery (filled contours), 150mb layer average of EPV*(sec⁻¹) less than 0.25 PVU, and frontogenesis (K/100km/3hrs, line contours) valid 15 Mar 2004 at (a) 12Z, (b) 18Z, and 16 Mar 2004 at (c) 00Z, and (d) 06Z.

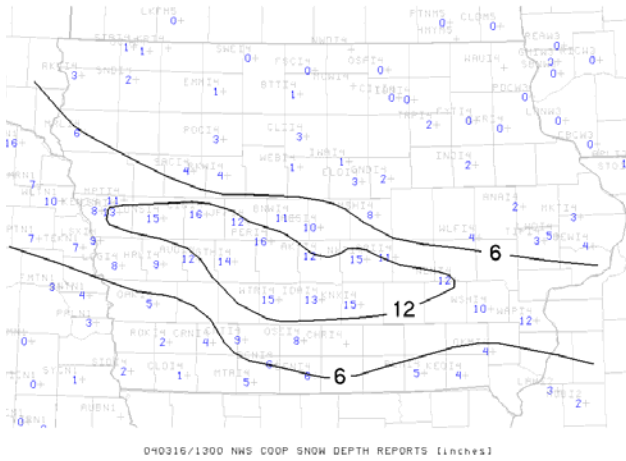


Fig. 4. Total snowfall (in) for 15-16 Mar 2004 across Iowa. (IEM)

At 12Z on the 15th, low pressure at the surface was stationed in south central Nebraska, with a warm front extending to the southeast. Warm air advection was strong ahead of the low, and a weak trough had developed at 500mb. This storm system was also associated with the right entrance region of a 300mb and 250mb jet streak. Composite radar showed a narrow band of snow from southeast South Dakota through southern Iowa. Frontogenesis locations at 700mb and 750mb were close, at 20km to the north and 39 km to the south of the snowband. A band of EPV* in the 750mb to 600mb layer was vertically juxtaposed and oriented quasi-parallel to the snowband and 750mb and 700mb frontogenesis. Also a deep layer of negative EPV* is located to the south (Fig. 3(a)).

The surface low moved southeast into northeastern Kansas by 18Z, with a snowband oriented from west to east across central Iowa. Frontogenesis at 800mb was closest to the snowband at 33km south, a bit lower in the atmosphere than at 12Z. MSI weakened slightly, but was present in the 850mb to 700mb layer, and was positioned well with respect to the 800mb frontogenesis and snowband. Negative EPV* values were confined to the southeast of the forcing (Fig. 3(b)). This layer of instability combined with the lift from frontogenesis at 12Z and 18Z fits the conceptual model proposed by Nicosia and Grumm (1999) (Fig. 1(a)) and may have resulted in the heavy snowband in this region.

At 00Z, the surface low continues to the southeast, centered along the Kansas-Missouri boarder. The 700mb frontogenesis maximum directly lined up with the radar indicated

snowband, once again positioned across central Iowa. Frontogenesis at 650mb and 750mb was within 30km to the north and south respectively. EPV* above these levels continued to become more negative south of the snowband and frontogenesis, and was well-collocated with a pronounced mid-level dry intrusion into the storm (Fig. 3(c)).

By 06Z, radar showed a residual band of snow in southeast Iowa. The surface low had shifted east, positioned in eastern Missouri and southern Illinois. Although frontogenesis was weak in all layers, the upper levels analyzed appear to have the best correlation with the snowband once again. The 600mb frontogenesis was directly aligned with the snowband. EPV* continued to remain negative south of the snowband (Fig. 3(d)). The orientation of the instability at 00Z and 06Z fits the conceptual model in Fig. 1(b).

This case showed that the level of frontogenesis in good agreement with the radar-indicated snowbands varied throughout the specified time periods. Early on, the snowband may have been directly associated with slantwise convection from the release of CSI above the mid-level frontogenesis. As the storm evolved, the slantwise and gravitational instability developed to the south, becoming collocated with the mid-level dry intrusion. The variable location of the instability verified both conceptual models presented in Fig. 1.

c. March 17-18, 2005



Fig. 5. Total estimated precipitation (in) for and 18 Mar 2005 across the upper Midwest. (NWS)

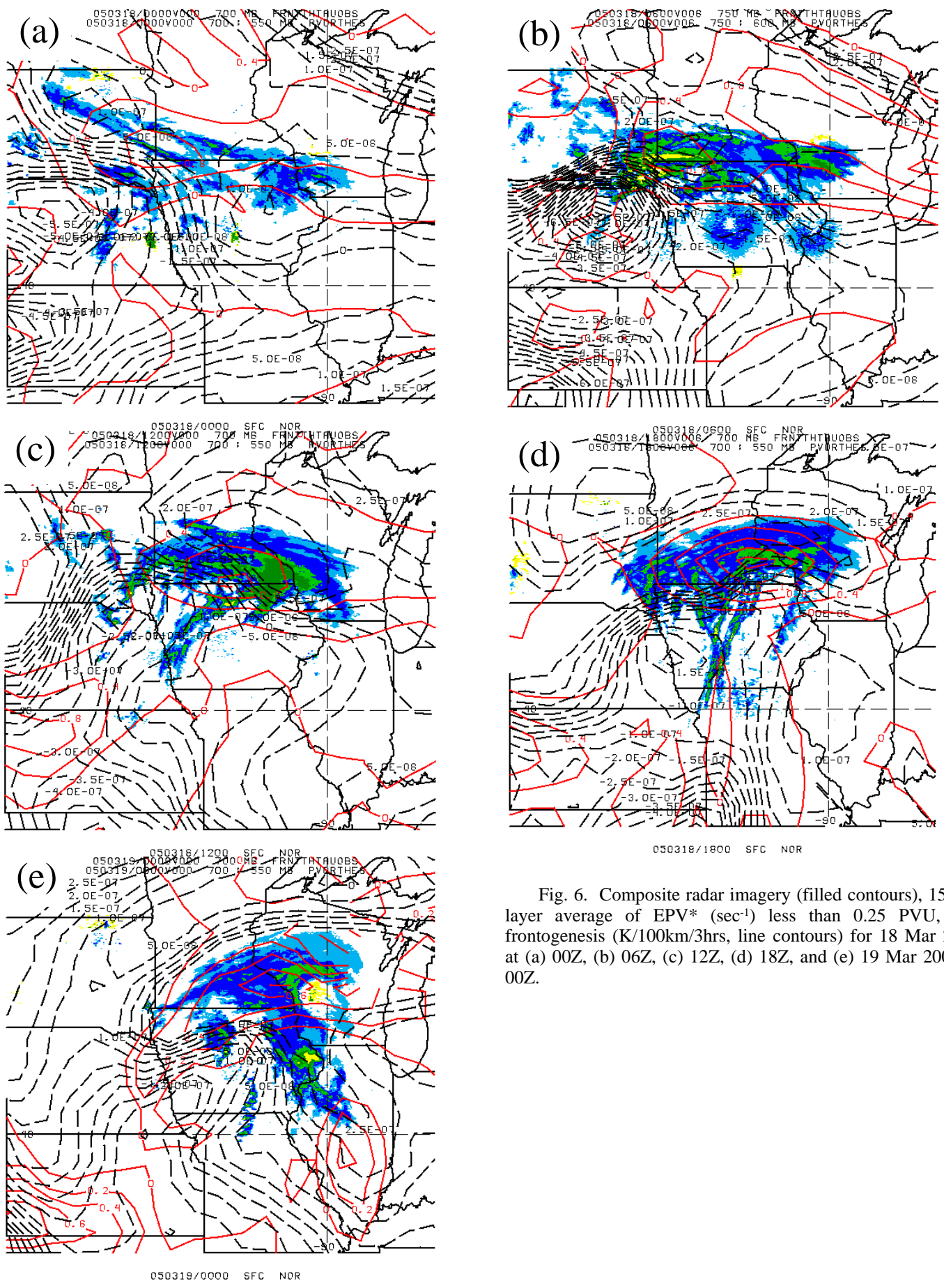


Fig. 6. Composite radar imagery (filled contours), 150mb layer average of EPV* (sec⁻¹) less than 0.25 PVU, and frontogenesis (K/100km/3hrs, line contours) for 18 Mar 2005 at (a) 00Z, (b) 06Z, (c) 12Z, (d) 18Z, and (e) 19 Mar 2005 at 00Z.

Heavy snow was reported on 17-18 March 2005 across southeast South Dakota and southern Minnesota, with twelve to sixteen inches of snow reported in this area (Fig. 5). Five time periods were selected for this case, from 00Z on the 18th through 00Z on the 19th.

At 00Z on the 18th, surface low pressure was centered well to the west in northeastern Colorado. A stationary front was aligned west to east across central Nebraska and Iowa, with a tight temperature gradient on either side of the front. These features were associated with a shortwave trough at 500mb, with positive vorticity advection also occurring in the region, and the left exit region of a weak upper-level jet streak. Composite radar showed a narrow band of snow occurring across eastern South Dakota and southern Minnesota. Frontogenesis at this time was weak, but well positioned at 700mb with respect to the snowband. EPV* values in the 700mb to 550mb layer were near zero, indicating weak symmetric stability, with negative values to the southwest (Fig. 6(a)).

The surface low made a northeasterly track into south-central Nebraska by 06Z, following the stationary boundary. Cold air advection was beginning to take shape behind the system, as an upper-level trough began to form. Frontogenetic forcing at 750mb and 800mb was closely associated with the snowband, slightly lower in the atmosphere than before. Once again, EPV* values were near zero above the 750mb frontogenesis, with negative values to the southwest and building to the southeast (Fig. 6(b)).

By 12Z, the surface low continued to move along the stationary boundary, positioned in northeastern Nebraska. Cold air advection continued to enhance behind the system, as a 500mb trough formed as well. Frontogenesis at 650mb, 700mb, and 850mb were aligned well with the snowband. This was slightly unusual to see multiple levels associated with the snowband. EPV continued to remain near zero above the 700mb frontogenesis, with the zone of negative EPV* persisting to the southwest of the snowband. Also of note, a small pocket of symmetric stability developed on the northeast side of the snowband (Fig. 6(c)).

The surface low took a more southeasterly path by 18Z and weakened. The trough at 500mb was well pronounced and nearly cutoff. Frontogenesis was well organized at this time, with a gradual slope of the frontal

structure with height. The 700mb frontogenesis maximum is in good agreement with the snowband location. The EPV* field took an interesting form when compared to radar and frontogenesis. Negative EPV* is once again positioned to the southwest, with near zero values lined along the southern edge of the snowband. Also, a pocket of symmetric stability took a similar shape to the frontogenesis maximum and snowband (Fig. 6(d)).

At 00Z, the surface low continued to weaken and move southeast into south-central Iowa. Frontogenesis was nearly vertical, with all maximums within 60km of the snowband. The pocket of symmetric stability in the 700mb to 550mb layer continued to take the shape of frontogenesis and radar valid at that time. Negative EPV* was still present to the southwest of the snowband (Fig. 6(e)).

This case illustrates the importance of using frontogenesis and EPV* to forecast heavy snow. Two of the time periods show that multiple levels of frontogenesis can be in close proximity to the snowband location. Also, the 700mb level consistently exhibits agreement with the snowband. Throughout this storm negative EPV* values were consistently located to the southwest of the snowband, and were likely associated with convective instability. EPV* values near zero positioned on top of, early on, and adjacent to, later on, the mid-level frontogenesis were likely associated with CSI. The emergence of a pocket of symmetric stability is also noted. This likely resulted from the release of MSI. Furthermore, this case provides evidence to validate both conceptual models presented in Fig. 1.

4. Results

Subsequent to calculating the distances, the data were imported into JMP 6.0 for analysis. In general, a shift from north to south occurred in the frontogenesis maximum as height decreased. This shift emphasizes that the frontal structure is tilted with height, and was present in all ten cases analyzed.

As the shift in the frontogenesis maximum occurs, the radar-indicated snowband becomes aligned with frontogenesis in the 700mb and 750mb levels. Table 1 indicates the 750mb and 700mb means are closest to the snowband, with the 600mb and 800mb means in

Table 1. Mean, median, and standard deviation (km) for the distance from the radar-indicated snowband to the frontogenesis maximum for each pressure level analyzed.

	Mean	Median	St. Dev.
600mb	56	65	75
650mb	14	33	69
700mb	10	0	81
750mb	-8	-39	109
800mb	-19	-33	89
850mb	-71	-83	116

close proximity. However, the standard deviation for all levels denotes a large spread in the data. Upon further analysis of the standard deviations, a trend is evident, revealing less variability of the snowband location with respect to the frontogenesis maximum as height increases. Table 1 and Fig. 7 illustrate that the mean for the 600mb, 650mb, 750mb, and 800mb levels is closer to the 0km line than the median of the data, signifying an outward skew of the data away from the snowband.

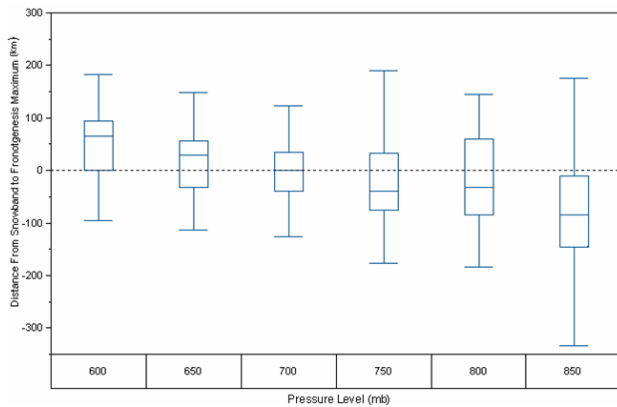


Fig. 7. Box and whisker plot for the distances (km) from the snowband to the frontogenesis maximum for each time period and pressure level analyzed.

Of the 38 time periods analyzed, the 700mb level was closest to the snowband 13 times, with the 750mb level closest only three times. The frontogenesis maximum at 700mb was within 40km of the snowband 21 of the 38 time periods. Additionally, the snowband and 700mb frontogenesis were directly aligned seven times, resulting in a median of 0km (Fig. 7). The 750mb frontogenesis maximum was within 40km of the snowband 14 of the 38 time periods, and was never directly aligned. This shows that more confidence can be placed in

analyzing frontogenesis at the 700mb level versus 750mb.

In the three cases analyzed in further detail, the level of frontogenesis aligned closest to the snowband varied with time. While the 750mb to 700mb range was close in 9 of the 13 time periods analyzed, the remaining 5 time periods showed large variability, wavering from 800mb to 650mb. Three of these five time periods were 6-hour forecasts, suggesting a small error may have been introduced by the model. However, the cumulative data set indicated that the 6-hour forecast showed no apparent relationship in consistently dislocating the 700mb to 750mb frontogenesis with the snowband. This indicates that the errors, if any, would be relatively small.

Additionally, all 13 time periods indicated the presence of negative EPV* aligned south of mid-level frontogenesis and the snowband. However, there appears to be no relationship between the orientation of EPV* and the radar-indicated snowbands. Also, the orientation of the precipitation is consistently aligned with frontogenesis in all 13 time periods.

5. Conclusions

The relatively small mean distance from the radar-indicated snowband to the frontogenesis maximum at the 650mb, 700mb, 750mb, and 800mb levels emphasizes the utility of frontogenesis in operationally forecasting heavy snow. The 700mb and 750mb means were in particularly close proximity to the snowband, suggesting improved confidence in using these levels to predict the snowband location. Additionally, it was shown that 700mb frontogenesis was more consistently collocated with the snowband than 750mb frontogenesis. This suggests that more confidence could be placed in this level. A layer average of these levels may provide a more accurate depiction of where the snowband will set up.

However, the standard deviations for all levels reveal a considerable spread in the data, which somewhat discredits the means to an extent. The spread in data may be due a number of factors known to vary spatially with time. This could include variability in which level of frontogenesis the moist symmetric instability was released, or changes in the location of the col point with height (Banacos 2003) among others. The exact answers are beyond the scope

of this study. Of the three cases analyzed in greater detail, three of the five times when frontogenesis was not collocated with the 700mb and 750mb levels occurred in the 6-hour forecast. This suggests that a small error may have been introduced by the model, and may have skewed the statistics slightly. However, the error was determined to be relatively small.

Furthermore, the standard deviations also show less variability in the data as height increases. Thus, rather than focusing strictly on the 700mb and 750mb means, a forecaster should then also look at 650mb frontogenesis. This level has the lowest standard deviation, which should more definitively show the snowband will be approximately 30-60km from the frontogenesis maximum on the warm side. Adjustments should then be made to resolve variations between these two approaches. If they agree, confidence in the forecast could be higher. It should be noted that this approach is based purely on statistics. A more scientific approach requires a thorough evaluation of parameters such as EPV*, deformation and col point, and the location of the trowal for example. From prior research, these factors have been shown to be in close association with banded precipitation.

Finally, both conceptual models are validated within two of the three cases analyzed in further detail, indicating a relationship between mid-level frontogenesis and the realization of MSI indicated by reduced EPV*. All 13 time periods support the conceptual model presented in Fig. 1(b), where reduced EPV* is adjacent to frontogenesis at mid-levels of the atmosphere. Furthermore, the 13 time periods indicate a relationship between the orientation of frontogenesis and the radar-indicated snowband, further emphasizing the utility of frontogenesis in the prediction of banded precipitation.

6. Acknowledgements

I would like to thank Daryl Herzmann for his help in acquiring and displaying data and Jon Hobbs for his assistance in statistical analysis.

7. References

American Meteorological Society, cited 2006:
AMS Glossary. [Available online at:

<http://amsglossary.allenpress.com/glossary/browse?s=f&p=45.>]

- Banacos, P. C., 2002: Frontogenesis forcing and banded precipitation. NOAA/NWS/WDTB WinterWeather Workshop. [Available online at: <http://www.wdtb.noaa.gov/workshop/WinterWx/index.html>.]
- _____, 2003: Short-range prediction of banded precipitation associated with deformation and frontogenetic forcing. *Preprints 10th Conference on Mesoscale Processes*, Portland, OR, Amer. Meteor. Soc.
- Bennetts, D. A., and B. J. Hoskins, 1979: Conditional symmetric instability—A possible explanation for frontal rainbands. *Quart. J. Roy. Meteor. Soc.*, **105**, 945-962.
- Browning, K. A., and T. W. Harrold, 1970: Air motion and precipitation growth at a cold front. *Quart. J. Roy. Meteor. Soc.*, **96**, 369-389.
- Dankers, T., 1994: Observing CSI bands using the WSR-88D. Postprints, *The First WSR 88D User's Conference*, Norman, OK, WSR-88D Operational Support Facility and NEXRAD Joint System Program Office, 159-168.
- Eliassen, A., 1962: On the vertical circulation in frontal zones. *Geo-phys. Publ.*, **27**, 1-15.
- Emanuel, K. A., 1983a: The Lagrangian parcel dynamics of moist symmetric instability. *J. Atmos. Sci.*, **40**, 2368-2376.
- _____, 1983b: On assessing local conditional symmetric instability from atmospheric soundings. *Mon. Wea. Rev.*, **111**, 2016-2033.
- _____, 1985: Frontal circulations in the presence of small moist symmetric instability. *J. Atmos. Sci.*, **42**, 1062-1071.
- Gall, R. L., R. T. Williams and T. L. Clark, 1988: Gravity waves generated during frontogenesis. *J. Atmos. Sci.*, **45**, 2204-2219.
- Grumm, R. H., and D. J. Nicosia, 1997: WSR-88D observations of mesoscale precipitation bands over Pennsylvania. *Natl. Wea. Dig.*, **21**, 10-23.
- Hobbs, P. V., T. J. Matejka, P. H. Herzegh, J. D. Locatelli and R. A. Houze, Jr., 1980: The mesoscale and microscale structure and organization of clouds and precipitation in midlatitude cyclones. I: A case study of a cold front. *J. Atmos. Sci.*, **37**, 568-596.
- Lindzen, R. S., and K. K. Tung, 1976: Banded convective activity and ducted gravity waves. *Mon. Wea. Rev.*, **104**, 1602-1617.

- Martin, J. E. 1999: Quasi-geostrophic forcing of ascent in the occluded sector of cyclones and the trowal airstream. *Mon. Wea. Rev.* **127**, 70–88.
- Moore, J. T., cited 2006: Banded heavy snow events. [Available online at <http://meted.ucar.edu/norlat/bandedsnow>.]
- Nicosia, D. J., and R. H. Grumm, 1999: Mesoscale band formation in three major northeastern United States snowstorms. *Wea. Forecasting*, **14**, 346–368.
- Sanders, F., and L. F. Bosart, 1985: Mesoscale structure in the Megalopolitan snowstorm of 11–12 February 1983. Part I: Frontogenetical forcing and symmetric instability. *J. Atmos. Sci.*, **42**, 1050–1061.
- _____, 1986: Frontogenesis and symmetric instability in a major New England snowstorm. *Mon. Wea. Rev.*, **114**, 1847–1862.
- Schultz, D. M., and P. N. Schumacher, 1999: The use and misuse of conditional symmetric instability. *Mon. Wea. Rev.*, **127**, 2709–2732.
- Schumacher, P. N., 2003: An example of forecasting mesoscale bands in an operational environment. *Preprints 10th Conference on Mesoscale Processes*, AMS, Portland, OR.
- Shields, M. T., R. M. Rauber, and M. K. Ramamurthy, 1991: Dynamical forcing and mesoscale organization of precipitation bands in a midwest winter cyclonic storm. *Mon. Wea. Rev.*, **119**, 936–964.
- Szeto, K. K., R. E. Stewart and C. A. Lin, 1988: Mesoscale circulations forced by melting snow. Part II: Application to meteorological features. *J. Atmos. Sci.*, **45**, 1642–1650.
- Wang, P., D. B. Parsons and P. V. Hobbs, 1983: The mesoscale and microscale structure and organization of clouds and precipitation in midlatitude cyclones. VI: Wavelike rainbands associated with a cold frontal zone. *J. Atmos. Sci.*, **40**, 543–558.
- Wolfsberg, D. G., K. A. Emanuel, and R. E. Passarelli, 1986: Band formation in a New England snowstorm. *Mon. Wea. Rev.*, **114**, 1552–1569.
- Xu, Q., 1989: Extended Sawyer–Eliassen equation for frontal circulations in the presence of small viscous moist symmetric stability. *J. Atmos. Sci.*, **46**, 2671–2683.